PHYSICAL REVIEW A VOLUME 19, NUMBER 2 FEBRUARY 1979

Electron-transfer reactions of fast Xe^{n+} ions with Xe in the energy range 15 keV to 1.6 MeV

R. J. Beuhler, L. Friedman, and R. F. Porter*
Chemistry Department, Brookhaven National Laboratory, Upton, New York 11973
(Received 9 August 1978)

Electron-transfer cross sections for the reactions of Xe^{n+} (n = 1–4) with Xe atoms have been determined as a function of projectile-ion kinetic energy in the range 15 keV–1.6 MeV. For Xe^{n+} (n = 2, 3, 4), cross sections for sequential transfer of two or more electrons in single-ion–atom collisions have been obtained. These cross sections decrease with increasing number of electrons transferred. The observed insensitivity of cross sections to projectile kinetic energy in the range investigated follows the condition that the linear velocity of the ion is less than the orbital velocity of a valence electron in the slow-moving target atom. Attenuation cross sections for reactions of Xe^{n+} (n = 2, 3, 4) follow approximately a $Z_{\oplus}^2$ charge dependence. A simple classical model based on Coulomb forces yields cross sections with a reasonable fit to the experimental data.

I. INTRODUCTION

Proposals to use heavy-ion beams to initiate controlled thermonuclear reactions have stimulated interest in xenon-ion–atom and ion-ion collision cross sections.[1] Information on ion-atom interactions, for ions with approximately 50-keV acceleration, is relevant to problems in the vicinity of the ion source and during very early stages of ion acceleration. Ion-ion interactions that may occur in the process of "bunching" accelerated ion beams, prior to impact on fuel-containing targets, may take place with ions of the same magnitude of relative energy, roughly 50 keV. These processes[2] are much more difficult to study experimentally because of the problem of producing number densities of low-velocity charged particles sufficient for the measurement of the desired interaction cross sections. However, the measurement of ionization of a xenon positive ion into a higher charged state by collision with a neutral xenon atom has been suggested as an approximation,[3] to the similar ionization in an ion-ion interaction, which may serve as a test of theoretical models used to estimate cross sections of the latter process.

The energy range of interest is, to the best of our knowledge, a subject that has not yet been investigated extensively. Experimental studies on argon-ion–atom collisions have recently been completed by Klinger and co-workers.[4] Theoretical studies of electron capture and loss processes in this energy range, in which ion velocities are slightly lower than orbital electron velocities, are difficult. Bohr's comment in 1948,[5] "For particle velocities of the same order of magnitude as the orbital velocities of the electron before and after its capture, neither classical mechanics nor the Born approximation can yield accurate results," may account for the apparent general lack of theoretical interest in these processes. The experimental results of Klinger and co-workers on electron capture by multiply charged argon ions showed rather large cross sections which were almost independent of velocity over the entire range of velocities studied. These results suggested that theoretical models developed to account for electron-capture processes at much higher ion velocities, with cross sections varying with as much as the inverse 12 power of projectile-ion velocity, were clearly inappropriate in the velocity range of interest. In view of the pessimism expressed by Bohr and the recent experimental data on the velocity independence of argon-ion electron-capture cross sections in the energy range 10–50 keV, it appeared that a systematic study of xenon-ion–atom interactions might provide information sufficient to justify the effort.

In this report we present the results of a study of xenon-ion–atom collision processes which include electron capture by singly and multiply charged xenon ions, data that overlap results of Klinger and co-workers on argon-ion–atom electron-capture processes, and some results on argon-ion-xenon-atom interactions. Measurements on the ionization of singly and multiply charged ions of xenon in collision with xenon atoms were also made because of their possible value in the estimation of ion-ion interaction cross sections. Studies were made with ions having velocities generally less than, but within an order of magnitude of, orbital electron velocities in the target atoms.

II. EXPERIMENTAL

The charge-transfer cross section experiments in this paper were performed with a 1.52-m radius, 90° magnetic isotope separator with a differentially pumped scattering chamber placed in either of two configurations behind the focal plane of the separator. Thus investigation of col-

lisions of ions with kinetic energies between 6 and 400 keV was made possible. The separator was built by the High Voltage Engineering Corp., Burlington, Mass. and has been described previously,[6] but we shall review some of the more critical features of the apparatus because of their bearing on the cross-section measurements.

The source of ions was a plasmatron ion source operated with an estimated pressure of 100 mTorr of rare gas. The arc voltage and current between the filament and ion-source housing were respectively, 70 V and 0.5 A for production of singly charged ions beams. Correspondingly higher arc voltages were used for more highly charged primary ion beams. The extraction voltage of the ions could be varied from ~10 to 50 keV and the magnetic field varied accordingly to provide a beam of variable energy at the focal plane of the separator. In all cases one isotopic peak of the primary ion beam was selected and the resolution $m/\Delta m$ of the separator was ~400. The intensity of the beam at the focal plane of ion collection was approximately 1 μA.

The apparatus described schematically in Fig. 1 was used for measurement of charge-transfer cross sections in the ion kinetic-energy range 10–50 keV. This system follows very closely the experimental arrangement first described by Fuls *et al.*[7] The entrance aperture (A in Fig. 1) to the collision chamber consisted of a 0.127-mm diam hole drilled through a 0.10-mm thick aluminum plate supported on a larger brass plate. Aperture B was a 1.0-mm hole beveled away from the collision chamber as shown in the figure. The two end plates of the collision chamber were separated by a brass tube into which a gas inlet and a pressure measurement tube had been silver soldered. The collision chamber assembly was then held together with a threaded rod assembly and vacuum epoxy was used to seal the chamber. The distance between apertures A and B was 8.9 mm. The pressure measurement was made with a MKS Baratron gauge, model 170M-6B, which was calibrated against a McLeod gauge. Experiments were generally carried out in a pressure range below a few mTorr to avoid multiple-collision processes.

Aperture C, 9.53 mm in diameter, was positioned 3.3 cm beyond B. The maximum observable scattering angle was 3.6°, fixed by apertures A and B. After C the particle beam entered an inhomogeneous electric field D having path length 4.5 cm. The purpose of D is to separate the different charged species resulting from charge-transfer collisions of the primary ions with the scattering gas. Typical deflection voltages between the plates were 10% of the primary beam energy.

The ion detection unit consisted of a Bendix M-306 electron multiplier mounted on a movable shaft. The multiplier slit was 2.54-mm wide and positioned 13.7 cm beyond aperture B. The usual

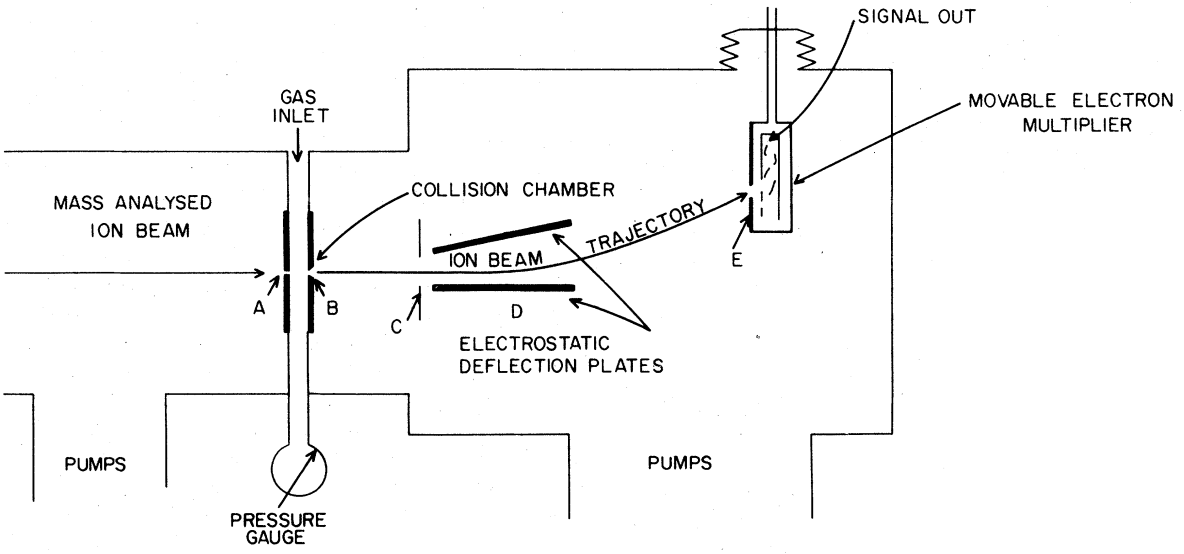

EXPERIMENTAL SCHEMATIC

FIG. 1. Experimental apparatus.

off-axis position was approximately 5 mm. Currents from the multiplier were measured on a Keithley model 410 A picoammeter. Typical beam signals were as follows. For the primary beam Xe^{1+} the signal was $\sim 2\times10^{-8}$ A with 1100 V on the multiplier. For the less intense multiply charged primary beams a multiplier voltage of 1400 V was used; the primary beams were then on the order of 1×10^{-8} A and scattered products approximately 10^{-10} A. During a run, with a particular primary ion beam, multiplier voltages were kept constant so that multiplier gain factors did not enter into the data analysis.

We assumed that equal fluxes of Xe^{4+}, Xe^{3+}, ..., Xe^{0} (all at the same velocity) would yield identical currents from the multiplier. This assumption was tested by making a series of charge-transfer measurements with the Bendix multiplier in the pulse-counting mode to compare with the results taken when the integrated response to a beam was being measured. The pulse counting mode is achieved at multiplier voltages of ~2000 V and incoming particle fluxes on the order of 10^4 counts/sec. Essentially no significant differences in pulse-height distributions from the respective separate species were observed.

To measure charge-transfer cross sections at ion kinetic energies up to 400 keV, the mass-analyzed beam from the isotope separator was focused through horizontal and vertical einzel lenses and entered a 34-stage, 93-cm long acceleration column. The scattering chamber and ion analysis system, similar to those items already discussed in Fig. 1, were positioned in a glass cross vacuum housing mounted at the high-voltage end of the column. For measurements at higher beam energies the electrostatic deflection plates were increased in length to 20 cm and the electron multiplier was repositioned approximately 30 cm behind the scattering chamber. Scattering pressures were kept below 2 mTorr which limited the pressure rise in the acceleration column to 8×10^{-7} Torr.

A polished aluminum dome enclosed the glass vacuum system at the end of the acceleration tube. The necessary electronics (Baratron, electron multipliers and deflection plate power supplies) and gas handling systems were placed inside this dome. Electronics inside the dome were powered by 110 V from a 400-keV isolation transformer. Fiber optical linkage controls were used to externally control the deflection plate power supplies. The scattering gas pressure was set for an entire series of runs and was read from the digital Baratron output observable through a hole cut in a panel of the high-voltage assembly. The ion intensities were measured in the pulse-counting mode as previously discussed and the pulse-counting rates were recorded on a strip chart recorder after transmission from the high-voltage assembly over a fiber optical linkage.

The power supply and isolation transformer were manufactured by the Universal Voltronics Corporation, Mt. Kisco, NY, model BRE-400-3 BNL. This supply is capable of delivering 3 mA at 0–400 keV in either polarity with 0.1% regulation and 0.01% rms ripple. Ion post-acceleration voltages were determined with an internal voltage divider within the power supply or an external voltage divider connected to a digital voltmeter. An independent check on these measurements was obtained from the magnitude of the deflection voltage required to bring the primary beam onto the electron multiplier which is a constant fraction of the total acceleration voltage. Measurements among all three different techniques were within 5% of each other.

III. RESULTS

Ion-atom reaction cross sections were obtained by two procedures. Attenuation cross sections (σ_a) were determined by measuring the fractional decrease in primary ion beam intensity when Xe was introduced into the collision chamber. For these experiments the electron multiplier detector was placed off-axis with respect to the exit aperture of the collision chamber. The attenuated ion beam was directed toward the detector by varying the voltage (V_d) on the deflection plates. This procedure was necessary to prevent fast secondary particles from reaching the detector when the primary beam was on axis. A second method of measurement involved determination of branching cross sections for each electron-capture or electron-loss process. For these measurements the multiplier was placed in a fixed configuration off-axis with respect to the collision chamber. Since the fast secondary ions retain the kinetic energy of the primary ion, their displacement from their normal trajectories will depend on V_d and ionic charge. Thus by sweeping the ion signal through a range of deflection voltages, the primary and secondary ion beams are resolved. For a stationary detector the extent of recorded ion deflection is directly proportional to the product ZV_d, where Z is the charge on an ion. Any pair of resolved ion signals appears with an intensity maximum corresponding to deflection voltages in the ratio $V_d'/V_d'' = Z''/Z'$. To obtain the correct relative ion intensities the integrated beam profiles must be multiplied by Z_s/Z_p, the ratio of charges on the secondary-primary ions. This normalization procedure is necessary because the

TABLE I. Experimental cross-section data for the process $Xe^{1+} + Xe \rightarrow Xe + Xe^{1+}$.

Ion energy (keV)	Pressure range (mTorr)	Number observations	σ_{1-0} (10^{-16} cm^2)
15	0.30– 4.2	4	23.9±2.6
20	0.23– 3.0	5	24.8±1.6
40	0.30– 2.4	5	23.1±1.4
50	0.135–2.15	5	25.2±1.9

width of a beam collected on the multiplier is inversely proportional to ion charge for constant incremental changes in V_d. When this correction is applied the resulting beam profiles of ions of varying charge have nearly identical halfwidths.

For measurement of cross sections for production of neutral particles (σ_{n-0}) the detector was located on the beam axis. The primary beam was first measured with collision chamber empty. Xenon was then introduced into the chamber and the primary beam was deflected away from the multiplier. Under these conditions the only signal detected was an undeflected beam of fast Xe atoms. All measurements were corrected for background residual gas scattering by subtraction of the very small signals observed in measurements with the collision chamber empty at initial base pressure conditions.

Attenuation measurements give an integral cross section for all interactive processes occurring in the collision chamber through the relationship

$$\ln(I_p^0/I_p) = \sigma_a nl,$$

where I_p^0 is the primary ion beam intensity, I_p is the attenuated beam intensity, n the number density of Xe atoms, and l the effective interaction path length which includes a correction for molecules leaving the collision chamber in the beam direction.[8] From beam deflection measurements we obtain the total primary beam intensity by summing the attenuated and secondary ion signals.

$$I_p^0 = I_p + \sum I_s .$$

From the relationship

$$\ln(I_p^0/I_p) = \sigma_t nl = \left(\sum \sigma_{n-m}\ nl\right),$$

we obtain an integral cross section for all reactive processes. This quantity is then fractionated into branching cross sections from the relative intensities of the secondary ions.

Our experimental procedure was tested against independently determined cross sections for reactions of Ar^{n+} with Ar(g).[2] For Ar^{1+} (50 keV) we find $\sigma_{1-0} = 10.6\times10^{-16}$ cm^2 compared with a value of 11.0×10^{-16} cm^2 reported by Fuls *et al.*[7] For 50-keV Ar^{2+} (Ref. 9) ions we obtain $\sigma_{2-1} = 9.7\times10^{-16}$ cm^2 which compares with a value of about 8.5×10^{-16} cm^2 estimated from data of Klinger and co-workers. Some preliminary experiments were performed to investigate the change in cross section as a function of the ion-source conditions. For example, lowering the source arc voltage to 20 V did not have an effect on the cross section in the case of σ_{1-0} for Xe^{1+} on Xe.

Results of our measurements are given in Tables I and II. We will discuss briefly results obtained for each Xe^{n+}-Xe reaction pair.

A. Xe^{1+}-Xe

The major process observed in the Xe^{1+}-Xe reaction is resonant-electron transfer. As we note

TABLE II. Summary of electron-capture and -loss cross sections for reactions of Xe^{n+} ions with Xe (units are 10^{-16} cm^2).[a]

Xe^{n+}	Ion kinetic energy (keV)	σ_a	σ_t	$\sigma_{n\rightarrow n-1}$	$\sigma_{n\rightarrow n-2}$	$\sigma_{n\rightarrow n-3}$	$\sigma_{n\rightarrow n-4}$	$\sigma_{n\rightarrow n+1}$
Xe^{1+}	50	26.7±2.9(7)	26.9± 2.3	25.2±1.9				1.7±0.4(8)
Xe^{2+}	100	24.6±2.5(6)	19.5± 1.5[b]	14.1±1.5(9)	5.4±0.1			
Xe^{3+}	150	54.9±5.4(12)	57.0± 4.2	37.8±2.8(7)	16.2±2.2(7)	2.9±0.2		
Xe^{4+}	200	86.3±6.3(7)	92.8±10.7	55.9±8.3(9)	29.7±3.8(9)	7.2±0.9(9)	~0.1	

[a] Number of observations indicated in parentheses; Xe pressure range was between 0.3 and 6.0 mTorr; values for σ_{n-0} were obtained graphically (Figs. 2 and 5).

[b] Contribution from σ_{2-3} not included.

from the data in Table I, σ_{1-0} was found to be insensitive to primary ion kinetic energies in the range of 15–50 keV. These data and the data plotted in Fig. 2 show that σ_{1-0} is essentially independent of collision chamber pressure below about 2.0 mTorr. A deflection profile from the Xe^{1+} primary beam at 340 keV is shown in the upper part of Fig. 3. Weak ion signals of Xe^{2+} and Xe^{3+} due to electron loss from Xe^{1+} are resolved in the spectrum. For primary ion beams of 340 and 50 keV, respectively, we obtain $\sigma_{1-2} = 2.1 \pm 0.5$ and $1.7 \pm 0.4 \times 10^{-16}$ cm^2. From one set of measurements at 340 keV we obtain $\sigma_{1-3} = (0.6 \pm 0.1) \times 10^{-16}$ cm^2. Attenuation cross sections for this system are quite close to the sum of σ_{1-0} and σ_{1-2}.

B. Xe^{2+}-Xe

The data in Fig. 2 indicate that σ_{2-0} is insensitive to Xe pressure below about 2.0 mTorr. The formation of Xe^{3+} by electron loss from 100-keV Xe^{2+} ions is evident in the asymmetry of the deflection profile on the primary ion signal (Fig. 4). An upper limit of $\sigma_{2-3} \leq 0.8 \times 10^{-16}$ cm^2 is set on this cross section. Attenuation cross sections for this system are slightly higher than the sum of σ_{2-1}, σ_{2-0}, and σ_{2-3}. A deflection profile from an 800-keV Xe^{2+} beam shows resolved secondary ion signals of Xe^{5+}, Xe^{4+}, and Xe^{3+} (Fig. 3). Electron-loss cross sections, σ_{2-3}, σ_{2-4}, and σ_{2-5}, obtained from these data are 1.5, 0.7, and 0.3×10^{-16} cm^2, respectively.

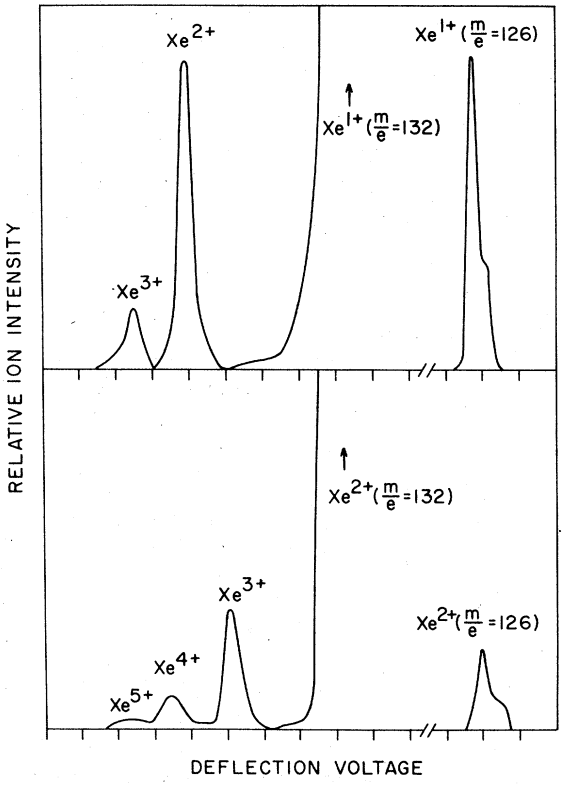

FIG. 3. Electrostatic deflection spectrum of ions resulting from interaction of Xe^{1+} ($m/e = 132$) with Xe(g). Primary ion intensity obtained by correcting intensity of Xe^{1+} ($m/e = 126$) for isotopic abundance, $^{132}Xe/^{126}Xe = 306.4$. Ionization of Xe^{1+} beam shown in upper part of figure, Xe^{2+} in lower part of figure.

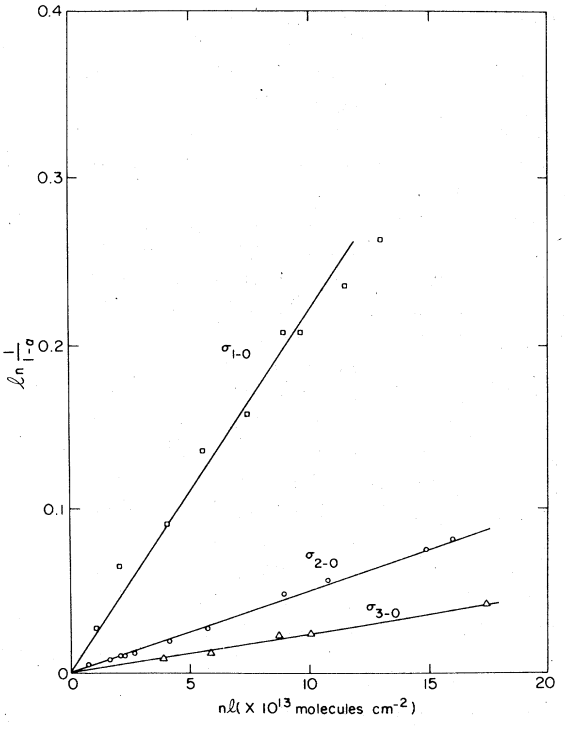

FIG. 2. Cross-section data for the processes $Xe^{m+} + Xe \rightarrow Xe^{0} + Xe^{m+}$. Slopes of curves equal σ_{m-0}. α is the ratio of intensities of fast neutral Xe atoms to unattenuated primary ion.

C. Xe^{3+}-Xe and Xe^{4+}-Xe

The extent of multiple-electron transfer in these systems is evident in the deflection profiles which show two capture processes for Xe^{3+} and three for Xe^{4+}. An apparent pressure dependence was observed only for σ_{4-0} (see Fig. 5). This is probably due to the formation of neutral Xe atoms by secondary collisions involving Xe^{3+} formed in the collision chamber. Extrapolation of the data in Fig. 5 to $P_{Xe} = 0$ gives a value of $\sigma_{4-0} = 0.1 \times 10^{-16}$ cm^2. The insensitivity of electron-capture cross sections to projectile energy is noted in Fig. 6. Attenuation cross sections are not distinguishable from total reaction cross sections within the limits of statistical error.

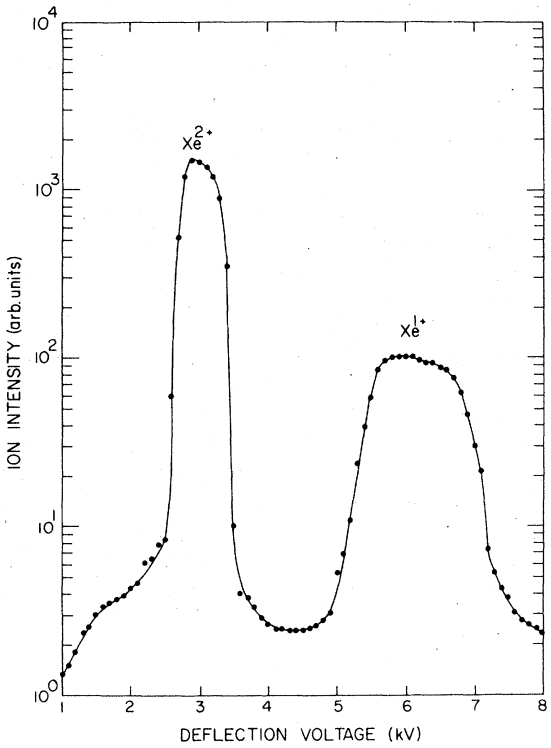

FIG. 4. Deflection spectrum of ions resulting from interaction of Xe^{2+} with $Xe(g)$.

IV. DISCUSSION

Results obtained in the study of charge-transfer and electron-capture reactions can be summarized as observations of relatively large cross sections relatively insensitive to ion kinetic energy in the energy range investigated (see Fig. 6). Cross sections for collisions of Xe^{n+} beams in the 50–200 keV kinetic energy range are presented in Table II. Comparison of electron-capture cross sections

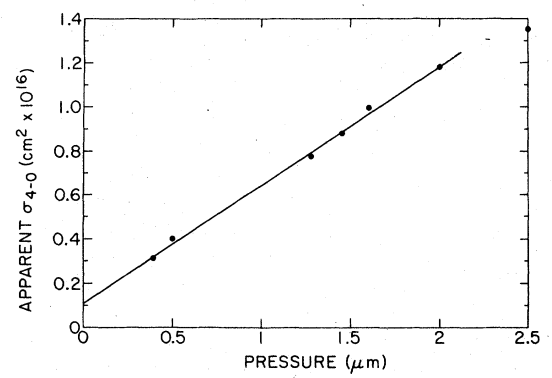

FIG. 5. Apparent dependence of σ_{4-0} on collision-chamber pressure.

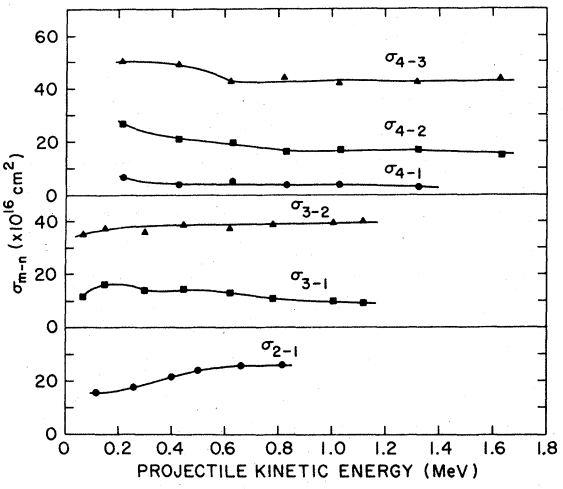

FIG. 6. Dependence of σ_{n-m} on kinetic energy of projectile ion.

of ions with different velocities or kinetic energies (in this energy range) is valid because of their observed insensitivity to velocity or kinetic energy. Similar observations were reported by Klinger and co-workers in their study of Ar^{n+} electron-capture processes.

Ion attenuation cross sections (shown in the third column of Table II) are almost completely accounted for by symmetric resonant charge transfer in the case of Xe^{1+} Collisional ionization of Xe^{1+} giving Xe^{2+} and Xe^{3+}, respectively, amounts to less than a few percent of the ion attenuation cross sections (Fig. 3). The symmetric resonant-charge-transfer cross section determined for 50-keV Xe^{1+} ions is approximately 30% larger than the value calculated by Rapp and Francis[10] using their semiclassical impact-parameter method. No serious consideration was given to the extension of the Rapp and Francis two-state impact-parameter model to symmetric resonant multielectron charge transfers or asymmetric single or multi electron-capture processes of Xe^{n+} ions. The latter asymmetric electron-capture reactions, which may be nonresonant or accidentally resonant processes, are always exothermic if reaction products are formed in ground internal energy states. This exothermicity is due to the progressively higher recombination energies of the multiply charged xenon ions. These energies for Xe^{1+}, Xe^{2+}, Xe^{3+}, and Xe^{4+} are 12.1, 33.3, 65.4, and 107 eV, respectively.[11] Table II shows that the symmetric resonant transfer of two or more electrons between Xe^{n+} and xenon atoms

$$Xe^{n+} + Xe^{0} \rightarrow Xe^{0} + Xe^{n+}, \quad n \geq 2$$

is a small cross-section process which decreases with increasing charge on the xenon ion.

The relatively small cross sections for collisional ionization of Xe^{1+} and Xe^{2+}, e.g., $Xe^{1+}+Xe^{0} \rightarrow Xe^{2+}+Xe^{0}+e$, are cited as evidence of the low probability of extensive conversion of projectile ion translational energy into internal energy in endothermic reaction processes. The distribution of energy in the products of exothermic electron-capture collisions cannot be determined in our experiments. It is reasonable to assume that with the larger impact-parameter electron-capture processes that most of the energy liberated would be deposited as internal energy in reaction products. It follows from this assumption that electrons will be captured in fairly high quantum states.

If one considers the densities of states available to electrons transferred in these strongly exothermic reactions it is possible to simplify calculations of capture cross sections. Reasonable estimates of electron-capture cross sections can be made by using the Landau-Zener method for the determination of the probability of pseudocrossing of potential energy curves. Olson and Salop[12] have developed an absorbing sphere model (unit probability of reaction for collision within a critical impact parameter), based on the Landau-Zener method. Olson and Salop assumed that for complex atomic or molecular-ion–molecule collision processes that there were a high density of curve crossings in the internuclear range around the critical distance of the impact parameter R_x. The Landau-Zener transition probability depends exponentially on the adiabatic splitting of the respective potential energy curves, of product and reactant systems, at the curve crossing and the difference in their slopes at R_x. The latter difference was estimated for electron captures by multicharged positive ions to be the slope of the repulsive Coulomb curve of the product system. The region of R_x was assumed to be at large internuclear distance, where the diabatic potential energy curve for the reacting-ion–neutral-atom was assumed to have zero slope. Olson and Salop then assumed that they could approximate the systems of interest as one-electron systems in which an active electron can move between relatively inert centers of charges $+1$ and $+z$, respectively. This assumption facilitates rapid calculation of relevant radial coupling matrix elements which give the adiabatic splitting parameters required for the application of the Landau-Zener method. While Olson and Salop commented that their method is most applicable to electron-capture reactions where z is large (≥ 10), their calculated cross section for Xe^{4+}-Xe^{0} reactions is in good agreement with our results.

An alternative approach is to use a model similar to the one devised by Bell[13] which accounts for electron capture and loss by gaseous fission fragments passing through a low-pressure gas. Bell's model assumes that the captured electron is liberated from its parent atom at ion-atom separations large compared to the dimensions of the ion or target atom. Thus the dominant force on the electron transferred in the capture process is the long-range Coulomb interaction between the ion charge and the electron. At a critical ion-atom distance R_x, the Coulomb force is equal to that binding the electron to its parent atom and the electron is liberated. For the ion velocity range of our experiments and collisions within R_x, Bell's model would predict unit probability of electron capture. An insensitivity of capture cross sections to projectile ion velocity up to a critical velocity slightly less than the velocity of the orbital electron in the target atom is also predicted. The critical distance of interaction for electron capture can be estimated by equating the Coulomb ion-electron potential to the ionization potential I_p of the atom so that

$$R_x = Ze^2/I_P$$

and

$$\sigma_t = \pi R_x^2 ,$$

where I_P is the ionization potential of the target atom and Z the charge on the projectile ion. We thus consider the long-range Coulomb interaction as taking place between a point-charge projectile ion and point-charge electron located effectively at the center of the target atom.

These critical distances should be proportional to the square root of the respective electron-capture cross sections if the assumptions of the classical model are correct. The results in Table II show attenuation cross sections roughly proportional to the square of the charge on the multicharged xenon ions. Comparison cross sections estimated using the classical model with experimental results is made in Table III. Data on Ar^{n+} reactions were taken from Klinger and co-workers.[4] The comparison of single-electron capture probabilities with total attentuation cross sections was based on the assumption of an electron-capture mechanism in which electrons are sequentially transferred from target to projectile species in one collision. The first electron transfer is postulated as occurring at the maximum critical distance of ion-atom interaction. Some ion trajectories will bring the projectile ion closer to the target species with the resulting transfer of a second or third electron. Such processes will deplete the observable concentration of single-electron capture products. Thus the total probability

TABLE III. Comparison of calculated and experimental cross sections for the reactions of Xe^{n+} with Xe and Ar^{n+} with Ar.

Xe^{n+}			Ar^{n+}		
n	σ(calc) (10^{-16} cm^2)	σ(expt) (10^{-16} cm^2)	n	σ(calc) (10^{-16} cm^2)	σ(expt) [a] (10^{-16} cm^2)
2	18	24	2	11	8.5
3	40	55	3	24	37
4	71	86	4	42	63
			5	66	65
			6	95	77
			7	129	101

[a] Data abstracted from Ph. D. thesis of H. Klinger (Justus Liebig University, Giessen, Germany, 1974). See also H. Klinger, A. Müller, and E. Salzborn, J. Phys. B 8, 230 (1975). Data corrected by E. Salzborn (private communication); contribution from σ_{n-0} not included.

of single-electron capture is measured by the sum of all capture cross sections.

This simple model predicts an identical cross section for capture of electrons by a variety of multicharged rare-gas ions in collisions with the same species of neutral rare-gas atoms. For example, the observation that Ar^{3+} ions in collision with Xe^0 neutral atoms gave results for one- and two-electron capture cross sections of 40 and 14.4×10^{-16} cm^2, respectively, similar to the Xe^{3+} on Xe^0 values of 37.8 and 16.1×10^{-16} cm^2, supports the assumptions of the model. Agreement between calculated values of electron-capture cross sections and experimental results obtained by Klinger and co-workers for Ar^{n+} on Ar^0 is not as good with significant discrepancies for Ar^{3+} and Ar^{4+} on Ar^0. Similar discrepancies are observed with Klinger *et al.* measurements on Ar^{n+} on Kr^0. However, the general trend of these cross sections is qualitatively predicted by a model assuming exclusively a Coulomb interaction between the projectile ion and an atomic electron. The success of this oversimplified model may be the result of a fortuitous cancellation of factors associated with the probability of exothermic electron capture by fast ions balanced by neglect of the finite size of the projectile ion and its polarization of electrons on the target atom. The classical model proposed above may be considered a one-electron model in which the critical value of curve crossing is evaluated by calculation of the distance at which the electron sees equal Coulomb attractions from its parent neutral atom and the projectile ion. The Olson-Salop application of the Landau-Zener method and the simple classical treatment differ in estimate of the z dependence of electron-capture cross sections. Classically, a z^2 dependence is predicted independent of the value of z. Presnyakov and Ulantsev[14] have developed a model which also gives a z^2 dependence of cross sections. Muller and Salzborn[15] have determined empirical scaling laws which provide a means of estimating electron-capture cross sections with an accuracy of approximately ±35%. Their empirical equation which contains three parameters, evaluated from study of beteween 30 and 100 experimental results, is an extension of the relatively simple model of Presnyakov and co-workers. The Olson-Salop semiempirical quantum treatment and the electron tunneling model of Grozdanov and Janev[16] predict a nearly linear dependence of cross section for capture of electrons by ions of high z ($z \geq 10$), in the velocity range of interest. Tests of the respective models will require more extensive experimental investigations of electron-capture processes.

ACKNOWLEDGMENTS

We wish to acknowledge the valuable technical assistance of Jory Yarmoff in carrying out these experiments. This research was carried out at Brookhaven National Laboratory under contract with the U. S. Department of Energy and supported by its Division of Basic Energy Sciences.

*On sabbatical leave from Cornell University.
[1]A. W. Maschke, BNL 5081T UC21, March (1978).
[2](a) G. C. Angel, K. F. Dunn, E. C. Sewell, and H. B. Gilbody, J. Phys. B 11, L49 (1978); (b) B. Peart, O. M. Gee, and R. T. Dolder, J. Phys. B 10, 2683 (1977); (c) J. B. A. Mitchell, K. F. Dunn, G. C. Angel, R. Browning, and H. B. Gilbody, J. Phys. B 10, 1897 (1977).
[3]Y. K. Kim, Argonne National Laboratory (private communication).
[4]H. Klinger, A. Muller, and E. Salzborn, J. Phys. B 8, 230 (1975).
[5]N. Bohr, K. Dan. Vidensk. Selsk. Mat.-Fys. Medd. 18, 8 (1948).
[6]T. F. Moran and L. Friedman, Rev. Sci. Instrum. 38, 668 (1967).
[7]E. N. Fuls, P. R. Jones, F. P. Ziemba, and E. Everhard, Phys. Rev. 107, 704 (1957).
[8]The effective interaction length is 11.57 mm based on a path length in the collision chamber of 8.9 mm and an estimated correction factor of 1.3 based on data in Ref. 4. Number densities were calculated with the ideal gas equation for a temperature of 300 K.
[9]The energy (volts) given for a particular ion refers to its kinetic energy rather than the acceleration potential.

[10]D. Rapp and W. E. Francis, J. Chem. Phys. 37, 2631 (1962).
[11]J. L. Franklin, J. G. Dillard, H. M. Rosenstock, J. T. Herron, K. Draxl, and F. H. Field, NSRDS-NBS, 29 June 1969.
[12]R. E. Olson and A. Salop, Phys. Rev. A 14, 579 (1976).
[13]G. I. Bell, Phys. Rev. 90, 548 (1953).
[14]L. P. Presnyakov and A. D. Ulantsev, Sov. J. Quantum Electron 4, No. 11, 1320 (1975).
[15]A. Muller and E. Salzborn, Phys. Lett. A 62, 391 (1978).
[16]T. P. Grozdanov and Janev, J. Phys. B 10, 1385 (1977).